IEEE Access
Multidisciplinary | Rapid Review | Open Access Journal

Received October 25, 2018, accepted November 24, 2018, date of publication November 28, 2018,
date of current version December 31, 2018.

Digital Object Identifier 10.1109/ACCESS.2018.2883750

Efficient Indoor Data Transmission With Full Dimming Control in Hybrid Visible Light/Infrared Communication Systems

XIAODI YOU[1,2], (Student Member, IEEE), JIAN CHEN[1], (Member, IEEE), AND CHANGYUAN YU[2], (Member, IEEE)

[1]School of Telecommunications and Information Engineering, Nanjing University of Posts and Telecommunications, Nanjing 210003, China
[2]Department of Electronic and Information Engineering, The Hong Kong Polytechnic University, Hong Kong

Corresponding author: Jian Chen (chenjian@njupt.edu.cn)

This work was supported in part by the National Natural Science Foundation of China under Grant 61271239 and in part by the Research Grant from The Hong Kong Polytechnic University under Grant HKPU 1-ZVL3.

ABSTRACT We design a hybrid visible light (VL) and infrared (IR) data transmission scheme for indoor visible light communication (VLC) systems with multi-pulse position modulation (MPPM) dimming control. A low-power IR light-emitting diode is adopted to assist the VL downlink especially when the dimming level of VL is low. Both VL and IR orthogonal frequency division multiplexing signals are transmitted alternately during the ''on'' and ''off'' periods of MPPM dimming controlled pulses. In this way, MPPM ''off'' periods can be efficiently utilized to convey data information without affecting illumination level. This arrangement ensures reliable data transmission under all illumination conditions including dark scenario. Numerical results show that the additional IR link can always facilitate the use of low M-ary quadrature amplitude modulation (M-QAM) levels. The fluctuation of required M-QAM symbol rates caused by dimming control can also be mitigated. At low dimming levels, both the receiver sensitivity requirement for the VL link and the total required transmit power can be significantly alleviated while maintaining a constant data rate at BER $< 10^{-3}$. Even with limited launching power, the proposed scheme can still extend dimming control range while achieving stable and reliable transmission quality effectively.

INDEX TERMS Visible light communication (VLC), infrared (IR) communication, dimming control, hybrid transmission, orthogonal frequency division multiplexing (OFDM), multi-pulse position modulation (MPPM).

I. INTRODUCTION

Recently, green indoor illumination has been considered as a significant portion of future urban infrastructure [1], [2]. Indoor visible light communication (VLC) using white light-emitting diodes (LEDs) has drawn worldwide attention [3]–[6]. Although indoor VLC features the dual functionality of illumination and data transmission, the former is the most basic purpose and should receive higher priority in system design. In practice, according to various application scenarios and different requirements of users, the illumination level of LED sources needs to be adjusted. Reducing the illumination level when necessary is also beneficial to energy conservation. Over the past few years, the topic of indoor VLC dimming control has gained extensive investigations [6]–[19]. Generally, the LED brightness can simply be controlled by using pulse width modulation (PWM) [8], [10]. The concept of PWM has been further extended in IEEE standard 802.15.7 [11]. However, due to the limited modulation bandwidth of LED devices, the capacity of VLC systems is usually constrained [20], [21]. Orthogonal frequency division multiplexing (OFDM), offering parallel transmission of high modulation formats through orthogonal subcarriers, can effectively increase LED bandwidth efficiency as well as overcome multi-path effects in indoor VLC [22]–[24]. Therefore, combining OFDM with dimming control has a bright future from the practical application perspective [13]–[15]. In [14], OFDM with variable M-ary quadrature amplitude modulation (M-QAM) was combined with PWM to improve transmission efficiency. However, under low illumination levels, both required symbol rate and receiver sensitivity requirement will be severely affected. A reverse polarity optical-OFDM scheme was reported in [15]. However, it is

2169-3536 © 2018 IEEE. Translations and content mining are permitted for academic research only.
Personal use is also permitted, but republication/redistribution requires IEEE permission.
See http://www.ieee.org/publications_standards/publications/rights/index.html for more information.

only applicable to inefficient unipolar forms of OFDM and will lead to a reduction of supported dimming control range. To achieve higher efficiency, schemes based on multi-pulse position modulation (MPPM) have been proposed in indoor VLC dimming control systems [16]–[19], [25]. Especially, in [19] OFDM was combined with MPPM, where different MPPM patterns can be utilized to transmit excess data information. However, under low dimming levels, both the required symbol rate and receiver sensitivity are still high, making it hard and inefficient to maintain stable link performance while conducting dimming control.

Nowadays, more and more applications are using invisible light sources at the infrared (IR) wavelength. Eye safety used to be of great concern for IR applications. However, according to the eye safety standards of IEC 60825-1, IR laser sources are actually permitted to transmit comparable optical power as compared with visible light (VL) laser sources [26]. On the other hand, with optical output power level up to Watts, IR LED products have been widely used in the fields such as night vision, cameras, traffic surveillance, biometrics, etc. According to the eye safety standards in IEC 62471, which is applied for lamps and lamp systems, the risk of IR LEDs with the emission limit of less than 100 W/m^2 can be exempted (wavelength: 780 nm∼1400 nm) [27]. Therefore, due to its relatively loose restriction in the safety standards, IR wavelengths can be utilized for indoor data transmission. IR based communication systems have been developed and reported in literatures [28]–[32]. In [33], through a VL or IR link, strategies were proposed for indoor Internet-of-Things applications, which achieved data transmission and power transfer simultaneously, with a solar panel at the receiver side. In addition, IR techniques are regarded as a potential uplink solution for future indoor VLC [34], [35]. Nevertheless, previous investigations on IR systems only focus on either a single downlink or a single uplink scenario. In current indoor VLC systems, there has been no investigation combining both VL and IR techniques together yet. Since IR is invisible and will not affect illumination, we can consider introducing IR techniques into VLC systems so as to assist the dimming control functionality.

In this paper, we present a novel VL/IR hybrid transmission scheme based on our previous reported VLC systems in [19] and [36]. An additional low-power IR downlink is adopted as a complement to the VL downlink. When dimming control happens, both the VL and IR DC-biased optical (DCO-) OFDM signals will be transmitted alternately within the ''on'' and ''off'' periods of MPPM patterns. Due to the invisible property of the IR link, this arrangement can provide sustained high-performance transmission while ensuring dimming control accuracy. As improvement with respect to previous works, each DCO-OFDM symbol will be transmitted via either a VL link or an IR link so as to guarantee stable transmission quality. In particular, a NOT gate in combination with two gate controlled switches are adopted at the transmitter side, helping avoid interference and keep synchronization for data demodulation. Therefore, it is simpler and more efficient for indoor VLC systems to implement dimming control. Extensive numerical simulations and comparisons are carried out respectively, which verify the effectiveness of the proposed scheme.

The rest of the paper is organized as follows. In Section II, the limitation of conventional schemes and the principle of our proposed hybrid transmission scheme will be presented in detail, respectively. Performance analysis will be provided in Section III. Numerical results and discussions will be given in Section IV. Finally, we provide a summary in Section V.

II. PRINCIPLE OF HYBRID VL/IR TRANSMISSION

A. LIMITATION OF CONVENTIONAL SCHEMES

As in [37] and [38], in this paper we ignore the faint indoor reflections from walls, ceilings, etc., and only consider a flat fading channel so as to focus on the dimming control issue. We assume the LED source to have a Lambertian radiation pattern. The channel DC gain is given as [30]:

$$H(0) = \frac{(l+1)\cos^l(\phi) S \cos(\psi)}{2\pi d^2}, \quad 0 \le \psi \le \psi_c, \quad (1)$$

where l is the Lambertian emission order of the transmitter, S is the physical area of the photo-detector (PD), d is the distance between the transmitter and receiver, φ is the angle of irradiance, ψ is the angle of incidence, ψ_c is the receiver field of view (FOV), respectively. The received carrier power can be given by:

$$P_r = H(0) P_t, \quad (2)$$

where P_t is the LED lamp power without modulation. At the output, the electrical signal-to-noise ratio (*SNR*) is written as:

$$SNR = \frac{(\gamma P_r m)^2 \overline{f(t)^2}}{\sigma^2}, \quad (3)$$

where γ is the responsivity of the PD, m is the modulation index of the LED transmitter, $f(t)$ is the normalized signal, respectively. The noise variance σ^2 consists of both shot noise and thermal noise. The noise bandwidth of a VLC system is consistent with the signal bandwidth at the receiver. Therefore, σ^2 is related to the received optical signal [19]. For conventional VLC systems adopting PWM or MPPM dimming control, OFDM data signals are only transmitted within the ''on'' periods of dimming controlled pulses. In order to maintain a data link with a constant capacity, the required M-QAM symbol rate needs to be inversely-proportional to a varying duty cycle D ($0 \le D \le 1$). As a result, the reduction of dimming level will cause an increase of required bandwidth, and in turn, lead to increased noise variance. This can be given as:

$$\begin{aligned}\sigma^2(P_r, R_0/D) &= \sigma^2_{shot}(P_r, R_0/D) + \sigma^2_{thermal}(R_0/D) \\ &= 2q\left[\gamma P_r\left(1 + m\overline{f(t)}\right) + I_{bg}I_2\right]R_0/D \\ &\quad + 8\pi k T_k \mu S (R_0/D)^2 \left(\frac{I_2}{G} + \frac{2\pi\Gamma\mu S I_3 R_0/D}{g_m}\right), \quad (4)\end{aligned}$$

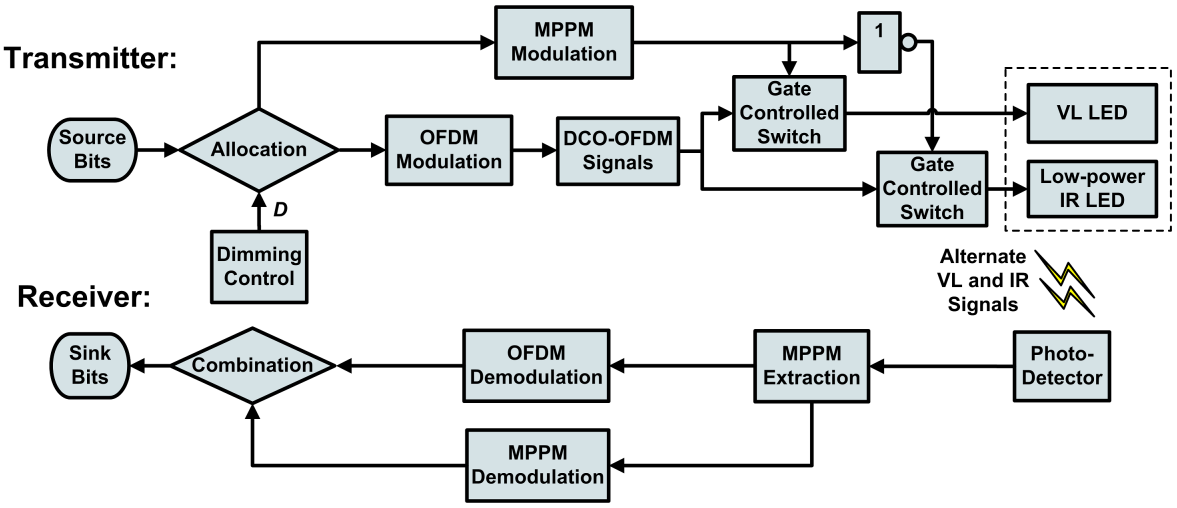

FIGURE 1. Block diagram of the proposed hybrid VL/IR data transmission system.

where R_0 is the initial symbol rate when D is equal to 1, q is the magnitude of electron charge, I_{bg} is the background current, both I_2 and I_3 are noise-bandwidth factors, k is the Boltzmann constant, T_k is the absolute temperature, g_m is the field-effect transistor (FET) transconductance, Γ is the FET channel noise factor, G is the open-loop voltage gain, and η is the fixed capacitance, respectively. According to [39], the upper bound of the BER for M-QAM can be theoretically given as:

$$BER \leq 0.2 \exp\left[\frac{-1.5\left(\gamma P_r m\right)^2 \overline{f\left(t\right)^2}}{\left(M-1\right)\sigma^2\left(P_r, R_0/D\right)}\right], \tag{5}$$

where M is the adopted M-QAM level. When adopting Reed-Solomon forward error correction (RS-FEC) code for the VLC system, BER of 10^{-3} is usually regarded as a reference value to achieve reliable transmission [40]. With dimming control, in order to maintain this targeted BER, the required receiver sensitivity for the VL link can be derived according to (5). When reducing dimming level, the required symbol rate needs to be increased to maintain a constant capacity, thus leading to increased receiver sensitivity. Therefore, with dimming control it will be difficult and inefficient to maintain a stable data link. In [19], although a method of combining OFDM and MPPM can alleviate this issue to a certain degree, performance improvement is not obvious under low dimming levels. The core issue is that previous schemes only used the "on" periods of dimming controlled pulses to convey data information, but did not effectively utilize the "off" periods. Therefore, when conducting dimming control, the required receiver sensitivity will be highly related to the varying duty cycle.

B. HYBRID VL/IR TRANSMITTER

In order to utilize the "off" periods of dimming controlled pulses efficiently, we propose to adopt a hybrid VL/IR transmission scheme, as presented in Fig. 1. When dimming control happens, the original data stream at the transmitter should be divided into two parts. One part is mapped to generate different MPPM dimming controlled patterns. Specifically, for each MPPM symbol with p pulses from a total of n slots (represented as (n, p) MPPM in the following part), the brightness level of the VLC system depends on the duty cycle D, where D is equivalent to p/n. The other part of the original data stream is modulated into DCO-OFDM signals, which will be fed into VL and IR LEDs alternatively. All these DCO-OFDM symbols will also be divided into two parts, which are transmitted within the "on" and "off" periods of MPPM patterns, respectively. During MPPM "on" periods, there only exists a VL link for data transmission. For this VL link, part of the total DCO-OFDM symbols, with the proportion to be $D^*100\%$, are controlled and transmitted according to modulated MPPM dimming controlled patterns. The MPPM patterns actually act as a control signal to manipulate a gate controlled switch for the VL link. As long as the state of MPPM is "1" level, the gate controlled switch will let the DCO-OFDM signals pass to modulate the VL LED. If the state of MPPM is "0" level, the switch is disconnect and there is no signal passed. As a result, these OFDM symbols are only transmitted within each MPPM "on" slot and will not modulate the IR LED source at all. Note that here the DC bias is assumed to be carefully arranged so that these DCO-OFDM signals are transmitted within the quasi-linear working range of the VL LED.

On the other hand, during MPPM "off" periods, there is only a low-power IR link which supports data transmission. This IR link is invisible and can be seen as an ideal complement to the influenced VL link due to dimming control. For this IR link, part of the total DCO-OFDM symbols, with the proportion to be $(1 - D) * 100\%$, are controlled and transmitted according to the inverse of MPPM dimming controlled pulses (or in other words, the "on" periods of inverse MPPM). These OFDM signals will not be used for

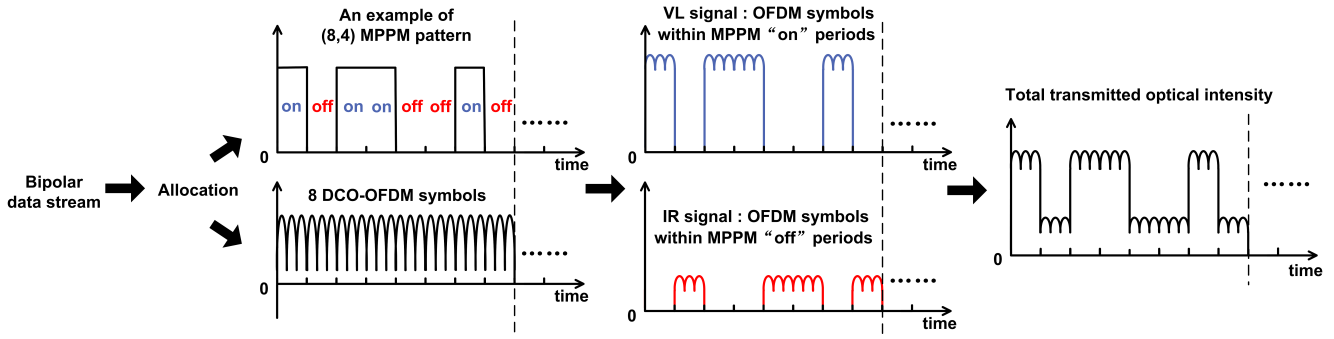

FIGURE 2. Schematic diagram of the signal waveforms in the time domain for both the VL and IR data links, respectively.

intensity modulation for the VL link either. The inverse of MPPM patterns can simply be realized by using a NOT gate. As a result, the "0" levels in MPPM "off" periods can be converted into the "1" levels. The inverse MPPM can also serve as a control signal for the IR link. Only when the state of inverse MPPM is "1" level, the gate controlled switch for the IR link will perform a turn-on operation so as to let the DCO-OFDM signals pass to modulate the IR LED. Adopting such a NOT gate also ensures that, both VL MPPM signals and IR inverse MPPM signals come from the same source of each MPPM pattern. This helps to maintain strict synchronization between both VL and IR signal branches, which is beneficial to signal demodulation at the receiver. In order for the convenience of extracting MPPM patterns at the receiver, the DC bias of the IR link should be kept relatively lower than that of the VL link. Therefore, for the IR link, the output of the gate controlled switch needs to be adjusted in advance of driving the low-power IR LED source. Finally, the hybrid signals consisting of VL DCO-OFDM and IR DCO-OFDM are transmitted alternately during the "on" and "off" periods of MPPM, together with MPPM patterns.

Note that this paper focuses on transmission of DCO-OFDM signals for proof-of-concept. Other OFDM schemes with high spectral efficiency, as in [41] and [42], can also be adopted in the OFDM branch of our proposed system, but at the cost of high complexity as well.

C. HYBRID VL/IR RECEIVER

The schematic diagram of signal waveforms in the time domain for both the VL and IR links are shown in Fig. 2, respectively. With dimming level to be 0.5, here we take a (8, 4) MPPM dimming controlled pattern as an example. As observed from Fig. 2, OFDM signals can be effectively transmitted via the IR link without affecting the dimming level of the VLC system. For hybrid VL and IR OFDM signals together with MPPM, synchronization can be maintained to avoid burst errors induced by signal crosstalk during demodulation. At the receiver, all signals will be detected by adopting a single PD. The detected hybrid electrical signal is then amplified, separated and demodulated according to subsequent digital signal processing. The output electrical signal at the receiver can simply be given by:

$$s(t) = \begin{cases} \gamma_{VL} P_{rON} \left(m_{VL} f\left(t\right) + 1\right) + n_{ON}\left(t\right), \\ \left(if\ MPPM\ \text{“}on\text{”}\ pulses\ are\ transmitted\right); \\ \gamma_{IR} P_{rOFF} \left(m_{IR} f\left(t\right) + 1\right) + n_{OFF}\left(t\right), \\ \left(if\ MPPM\ \text{“}off\text{”}\ pulses\ are\ transmitted\right). \end{cases} \tag{6}$$

Here $n(t)$ is the noise amplitude. In this paper, we adopt the subscript of VL/IR to distinguish the physical parameters for VL/IR links, respectively. We also adopt the subscript of ON/OFF to distinguish the physical parameters within the "on/off" periods of MPPM, respectively. From (6), the discrete output in slot q can be then written in the form of integration:

$$s_q = \frac{1}{T_s} \int_{(q-1)T_s}^{qT_s} s\left(t\right) dt, \quad q = 1,\ 2,\ 3,\ \cdots, \tag{7}$$

where T_s is the sampling interval.

Due to the huge difference between the VL and IR links in terms of received optical intensity, we can propose to adopt the following procedures to demodulate the hybrid signals: (Step i) Integrating received signal amplitudes within each discrete time slot; (Step ii) Extracting the maximum p pulses within every (n, p) MPPM pattern as MPPM "on" periods so as to demodulate MPPM; (Step iii) Classifying the received DCO-OFDM time domain symbols from both VL/IR links, respectively, according to the MPPM "on/off" states obtained in Step ii; (Step iv) Performing fast Fourier transform (FFT) to demodulate the classified VL and IR OFDM symbols, respectively; and (Step v) Decoding M-QAM signals and merging all data streams from OFDM and MPPM so as to recover the original data.

The extraction of MPPM in Step ii is the key procedure to distinguish VL and IR signals, respectively. According to (6), the threshold can simply be set as: $(\gamma_{VL} P_{rON} + \gamma_{IR} P_{rOFF})/2$. Then the recovered MPPM "on/off" states can inherently provide synchronization information for the combination of all signals including VL OFDM, IR OFDM, and MPPM itself. Here notice that the OFDM symbol length is less than or equal to MPPM chip duration, and there will be no latency problem. However, if the OFDM symbol length is larger than

MPPM chip duration, then each OFDM symbol will be transmitted across several discontinuous MPPM "on" or "off" states. This will result in transmission latency up to several OFDM symbol periods and other problems, which is not recommended. At the receiver side, channel state information is required to demodulate OFDM signals for both VL and IR links. The channel priori knowledge can be obtained based on the average of several recent received OFDM symbols in the time domain. Measurement can also be conducted by using the pilot in advance of actual data transmission. To extract MPPM, we can also consider adopting the scheme in [43], where detection of MPPM pulse transition is accomplished by finding the local maxima/minima of the first derivative of $s(t)$ in (6) [44].

III. PERFORMANCE ANALYSIS

The VLC channel model can be adopted in IR based systems [45], [46]. The only difference lies in different surface reflections at different wavelengths. Therefore, in the proposed IR link, we also deal with the LOS channel as that in (1). With the Lambertian property of the IR LED source, the eye safety issue is of no great importance. However, for the IR source with a narrow FOV, e.g., the IR laser, the eye safety issue should be considered for the additional IR link. During MPPM "on" periods, the received VL carrier power can be written as:

$$P_{rON} = P_{rVL} = H_{VL}(0) P_{tVL}. \tag{8}$$

After filtering the DC component, the electrical *SNR* of the VL signal at the output can be given as:

$$SNR_{ON} = \frac{(\gamma_{VL} H_{VL}(0) m_{VL})^2 P_{tVL}^2 \overline{f(t)^2}}{\sigma_{ON}^2}. \tag{9}$$

Here the noise variance σ_{ON}^2 includes both shot and thermal noise. Actually, σ_{ON}^2 is related to the new required M-QAM symbol rate R_1 as well as the VL carrier power P_{rVL}, which can be written as:

$$\begin{aligned}
&\sigma_{ON}^2(P_{rVL}, R_1) \\
&\quad = \sigma_{ON,shot}^2(P_{rVL}, R_1) + \sigma_{ON,thermal}^2(R_1) \\
&\quad = 2q\left[\gamma_{VL} P_{rVL}\left(1 + m_{VL}\overline{f(t)}\right) + I_{bg} I_2\right] R_1 \\
&\qquad + 8\pi k T_k \mu S R_1^2 \left(\frac{I_2}{G} + \frac{2\pi\Gamma\mu S I_3 R_1}{g_m}\right).
\end{aligned} \tag{10}$$

During MPPM "off" periods, the received carrier power only contains the IR component, which is given by:

$$P_{rOFF} = P_{rIR} = H_{IR}(0) P_{tIR}. \tag{11}$$

Due to the low launching power of the IR link, we can use κ to denote the ratio of intensity between both IR and VL links. This relationship can be written as $\kappa = P_{tIR}/P_{tVL}$. Here a small value of κ such as 0.1 should be used to facilitate the receiver distinguishing between VL and IR signals, respectively. Therefore, the relationship can be established by:

$$P_{rIR} = \kappa P_{rVL} H_{IR}(0) \big/ H_{VL}(0). \tag{12}$$

After filtering the DC component, the electrical *SNR* of the IR signal at the output can be given as:

$$SNR_{OFF} = \frac{(\gamma_{IR} H_{IR}(0) m_{IR})^2 P_{tIR}^2 \overline{f(t)^2}}{\sigma_{OFF}^2}. \tag{13}$$

Here the noise variance σ_{OFF}^2 in terms of R_1 and P_{rVL} can be represented by:

$$\begin{aligned}
&\sigma_{OFF}^2(P_{rVL}, R_1) \\
&\quad = \sigma_{OFF,shot}^2(P_{rVL}, R_1) + \sigma_{OFF,thermal}^2(R_1) \\
&\quad = 2q\left[\gamma_{IR}\kappa P_{rVL}\left(1 + m_{IR}\overline{f(t)}\right) H_{IR}(0) \big/ H_{VL}(0) + I_{bg} I_2\right] R_1 \\
&\qquad + 8\pi k T_k \mu S R_1^2 \left(\frac{I_2}{G} + \frac{2\pi\Gamma\mu S I_3 R_1}{g_m}\right).
\end{aligned} \tag{14}$$

Then according to [39], the upper bound of the BER in the proposed hybrid VL/IR system with dimming control can be given as:

$$\begin{aligned}
BER \le 0.2 \Bigg\{ &D \exp\left(\frac{-1.5 SNR_{ON}}{M_{VL} - 1}\right) \\
&+ (1 - D) \exp\left(\frac{-1.5 SNR_{OFF}}{M_{IR} - 1}\right)\Bigg\}.
\end{aligned} \tag{15}$$

Here the DC bias of the VL link is assumed to be much higher than that of the IR link. Therefore, both the high peaks of OFDM waveforms and the additive noise are relatively weak so that we can simply ignore their influence. With RS-FEC code, the required receiver sensitivity of the VL link P_{senVL} at the targeted BER of 10^{-3} can be therefore estimated according to the following expression:

$$\begin{aligned}
10^{-3} = 0.2D &\exp\left[\frac{-1.5 SNR_{ON}(P_{senVL}, R_1)}{M_{VL} - 1}\right] \\
&+ 0.2(1 - D) \exp\left[\frac{-1.5 SNR_{OFF}(P_{senVL}, R_1)}{M_{IR} - 1}\right].
\end{aligned} \tag{16}$$

Note that here both SNR_{ON} and SNR_{OFF} are actually related to the received optical signal in terms of R_1 and P_{senVL}, respectively. In (16), there exists a constraint between the dimming level, required M-QAM level, required symbol rate, and receiver sensitivity requirement. However, compared with conventional dimming control schemes, the unoccupied "off" periods of dimming controlled pulse can be effectively exploited by adopting the IR link. As a result, reducing dimming level will bring much less impact on both required M-QAM symbol rate and receiver sensitivity requirement, especially under low dimming levels. This makes it much easier and more power-efficient to maintain a reliable and stable data link under the dimming control scenario.

IV. SIMULATION AND DISCUSSIONS

In this section, a part of indoor VLC system parameters are listed in Table 1. They are kept consistent with conventional schemes as in [14] and [19, Table 1] for the purpose of performance evaluation and comparison. Except for Fig. 9, we assume the intensity ratio κ between IR and VL links to

TABLE 1. Parameters of indoor VLC system configuration.

Symbol	Description	Value
l	Transmitters' Lambertian emission order	1
S	Physical area of the PD	10^{-4} m^2
ψ_c	FOV at the receiver	170 deg.
I_{bg}	Background light current	5100 μA
I_2 / I_3	Noise-bandwidth factor	0.562 / 0.0868
g_m	FET transconductance	30 mS
Γ	FET channel noise factor	1.5
μ	Fixed capacitance	112 pF/cm^2
G	Open-loop voltage gain	10
T_k	Absolute temperature	298 K

be 0.1. The LED modulation index and the PD responsivity are assumed to be 0.2 and 0.5, respectively, for the VL link. In order to conduct a fair comparison with conventional dimming control methods, the configuration parameters of the IR link will be consistent with that of the VL link in Figs. 3, 4, 5, 6, 7 and 9. In this way the performance improvement attributed to the proposed additional IR link can be shown more clearly. For Figs. 10, 11 and 12, the parameters for the IR link will be adjusted for a further investigation. The room size is assumed to be 5 m × 5 m × 3 m (length × width × height). Since the data links are deployed in the presence of external background light, the background light current is considered, which adds to shot noise. Without loss of generality, the locations of LED lamps and the user are assumed to be (2.5, 2.5, 3.0) and (3.75, 1.25, 0.85), respectively. The light sources for both VL and IR links are assumed to be installed in the same location with the same Lambertian radiation pattern. Therefore, both VL and IR signals will experience the identical channel DC gain. Actually, for both links, as long as we obtain their channel DC gains in advance, both VL and IR LED sources can be installed at anywhere. The synchronization for signal demodulation can also be maintained. In this paper, the adopted PD is assumed to have a very wide range of spectral response, which covers both VL and IR

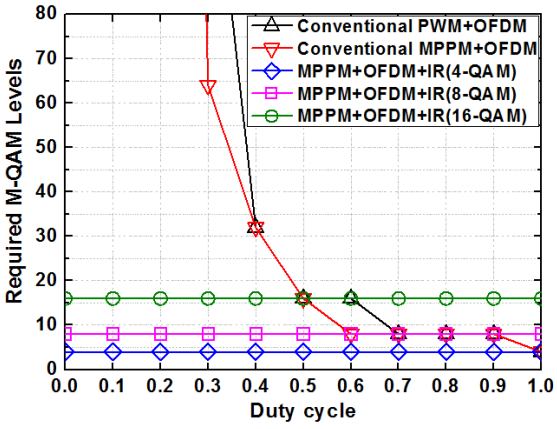

FIGURE 3. Comparison of the required M-QAM levels to maintain a constant consolidate transmission rate.

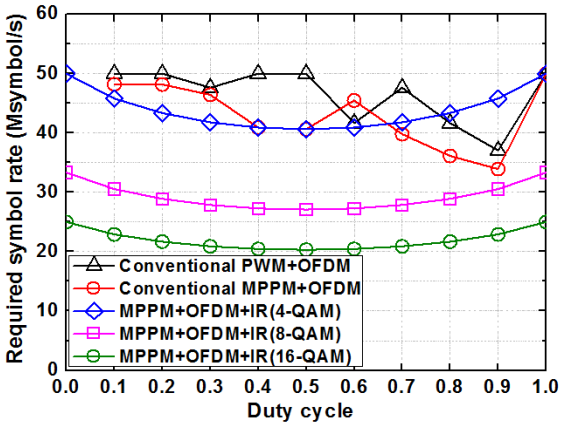

FIGURE 4. Comparison of the required M-QAM symbol rate to maintain a constant consolidate transmission rate.

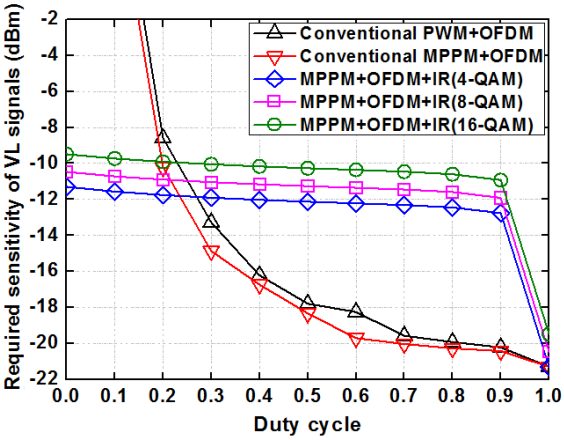

FIGURE 5. Comparison of the required sensitivity for the VL link.

wavelengths. This assumption is reasonable because quite a few kinds of PDs (e.g., Thorlabs FDS010, Thorlabs FD11A, Osram BPX65, First Sensor PS0.25-5-TO52S3) have this property. Accordingly, the near IR wavelength in the range between around 800 nm and 950 nm can be selected for the IR link. In practical scenarios, different wavelengths will show different PD responsivities. Adopting a single PD to receive both VL and IR signals may result in a variation of received signal levels. Therefore, the procedure of classification needs to be used. An alternative approach is to use optical band-pass filters at specific wavelength bands, where the wavelength selectivity property of a PD is utilized for performance improvement [5]. However, in this case two PDs are required in the hybrid system, but at the cost of increased system complexity. This is mainly due to the requirement of synchronization between two receiving branches.

In the proposed hybrid system, the dimming control process is represented by decreasing duty cycle from 1 towards 0. The system consolidate rate, initially set at 50 Mbps, is assumed to be constant during the entire dimming control range. When the dimming level D is 100%, DCO-OFDM

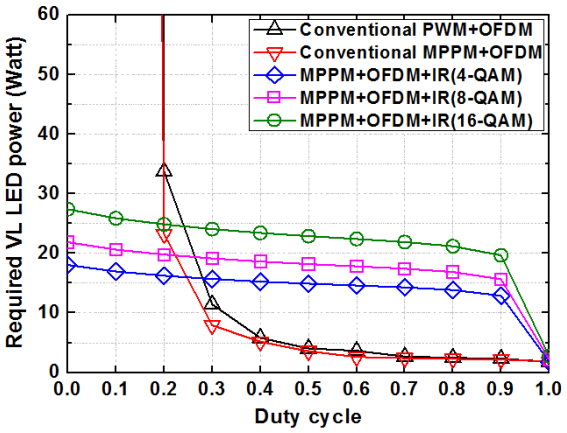

FIGURE 6. Comparison of the required launching power for the VL LED.

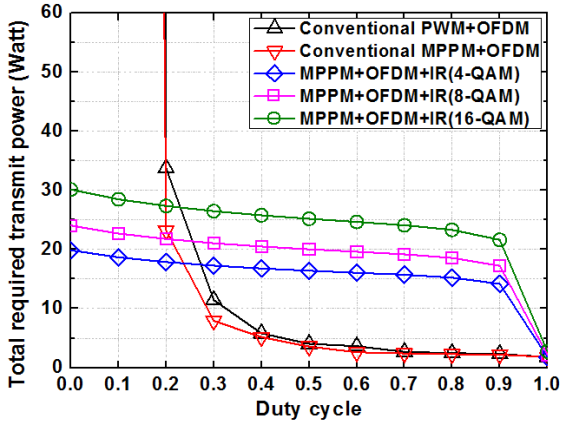

FIGURE 7. Comparison of the total required transmit power.

signals are simply transmitted via full PWM signals. When dimming control happens, each PWM period will be divided into a MPPM symbol. For the VLC link at a constant transmission rate, the required LED launching power needs to be minimized for the purpose of energy conservation. Accordingly, for different duty cycles, the adopted M-QAM levels should also be optimized so as to minimize the receiver sensitivity requirement of the VL signal. Based on the constraint of (16), the optimum M-QAM levels and corresponding M-QAM symbol rate to maintain a constant data rate under different dimming levels have been depicted in Figs. 3 and 4, respectively. From Fig. 3, for conventional PWM and MPPM systems, the required M-QAM levels will experience a rapid increase towards the reduction of illumination level so as to achieve a stable transmission rate. For instance, the required M-QAM level at D of 0.1 is calculated to be 1048576. Such a large value is practically unavailable. Besides, the range of dimming level is also limited, i.e., from 1 to around 0.3 or 0.4. Actually, at D of 0, there is no connectivity via the VL link (i.e., the VL LED light source is switched-off). Therefore, to maintain the most basic connectivity of the VLC system, an extra data link should be established on the basis of conventional schemes. However, by adopting the proposed hybrid transmission scheme, we can significantly reduce the required M-QAM levels. All the modulation formats such as 4-, 8-, and 16-QAM can be effectively used within a full dimming control range as compared with previous schemes. Besides, adopting constant M-QAM levels can also avoid the use of adaptive variable M-QAM in the entire dimming control range. In Fig. 4, while maintaining a constant data rate, the required M-QAM symbol rate can be significantly reduced when adopting an additional IR link, especially for 8-QAM and 16-QAM. Besides, compared with conventional schemes, the required symbol rate will not dynamically fluctuate due to dimming control. For example, for 4-QAM the required symbol rate with dimming control will be equal to or less than the initial symbol rate of 50 Mbps, but larger than 80% of it. These make the dimming control scheme easy to implement. In addition, when determining the M-QAM level adopted during transmission, we can refer to Fig. 4 and select the most suitable level so as to make sure the symbol rate range matches the VLC system. With a constant transmission rate, a lower required symbol rate usually indicates a higher M-QAM level.

Corresponding to Figs. 3 and 4, the required receiver sensitivity for the VL link, required VL LED launching power, and total required transmit power versus duty cycle are depicted in Figs. 5, 6 and 7, respectively. From Fig. 5, in conventional PWM and MPPM schemes, the receiver sensitivity requirement for the VL link will increase rapidly along with reduced dimming levels. For instance, the required receiver sensitivity is around -20.4 dBm at the dimming level of 0.9. For dimming levels from 1 to 0.3, MPPM can provide lower receiver sensitivity requirement than other schemes. However, adopting lower values of dimming level will lead to a sharp increase of receiver sensitivity requirement. This mainly results from increased M-QAM levels as in Fig. 3. Actually, in practical VLC systems based on PWM or MPPM, in order to achieve reliable communication quality, the required LED launching power should remain constant within the entire dimming control range from 1 to 0. Therefore, for conventional schemes, implementing dimming control is inefficient and hard, because quite a high launching power at low dimming levels needs to be adopted to satisfy the receiver sensitivity requirement under all illumination levels. However, the proposed hybrid system which combines 4-, 8- and 16-QAM OFDM with MPPM patterns can offer a much more flat receiver sensitivity response within the entire dimming control range. Here the required receiver sensitivity with 4-QAM is lower than that with 8- and 16-QAM. Therefore, for consideration of energy conservation, 4-QAM is more preferred. In Fig. 6, we also observe a similar trend of the required launching power P_{tVL} for the VL LED as in Fig. 5, along with reduced D.

Next, in Fig. 7, we compare the total required transmit power P_{tTotal} versus the varying duty cycle. For the proposed hybrid system, $P_{tTotal} = P_{tIR} + P_{tVL}$. These plots show a similar property as that in Figs. 5 and 6. From Fig. 7,

by adopting the low-power IR link as a complement, the total required launching power of the VLC system can be effectively reduced under low dimming levels (more specifically, for $0 \leq D \leq 0.2$). For instance, when D is equal to 0.1, P_{tTotal} is required to be 18.7 W, 22.7 W and 28.5 W for 4-, 8-, and 16-QAM, respectively. Actually, when D is equal to 0, there is no VL link at all. Only an IR link is active with the launching power of 1.81 W for 4-QAM. Therefore, if we want to achieve a constant transmission rate at BER $< 10^{-3}$ within the entire dimming control range, P_{tTotal} of 18.7 W is sufficient for 4-QAM. It can simply be calculated that the transmitted IR LED power in such hybrid system is far less than the emission limit of 100 W/m^2 according to the eye safety standards [27]. From Fig. 7, in order to achieve the minimum total transmit power P_{tTotal} in the full range of dimming levels, we also propose a mechanism as shown in Fig. 8. This mechanism can adaptively select different dimming control schemes according to the targeted duty cycle. For example, if the current duty cycle is no less than the preset switchover point D_s (i.e., 0.3 in Fig. 7), adopting conventional schemes can achieve both reliable transmission and energy conservation at the same time. If the current duty cycle is less than D_s, the proposed VL/IR hybrid scheme should be adopted to further reduce the receiver sensitivity requirement.

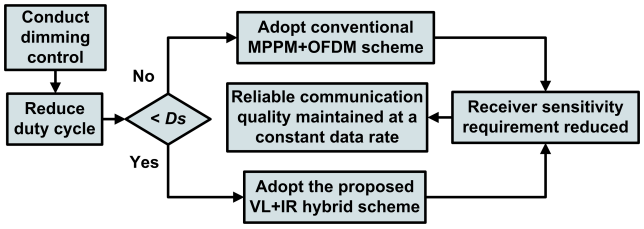

FIGURE 8. Mechanism to select different data transmission schemes adaptively.

Considering different values of κ, Fig. 9 shows the required transmit power for both VL and IR links, respectively. For the VL LED source, P_{tVL} is lower when using larger values

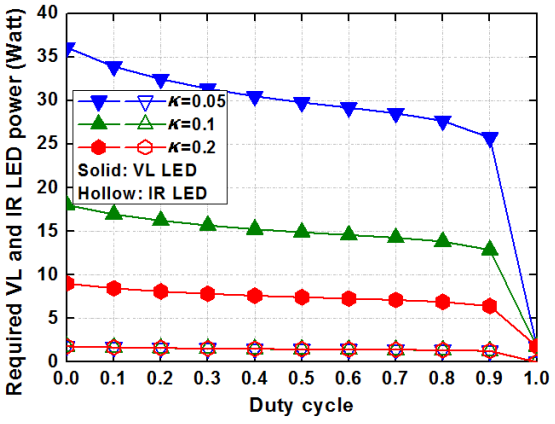

FIGURE 9. Comparison of the required LED power for both VL and IR links considering different values of κ.

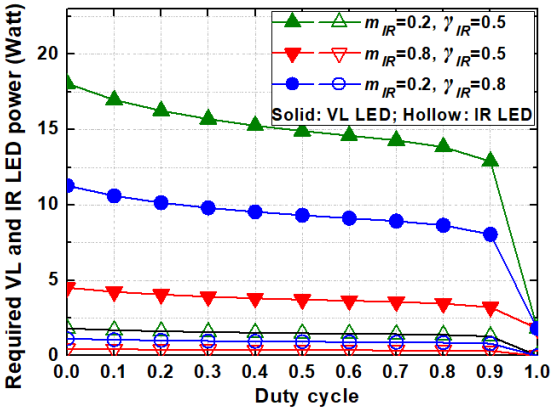

FIGURE 10. Comparison of the required LED power for both VL and IR links. Here different modulation indexes and PD responsivities for the IR link are considered.

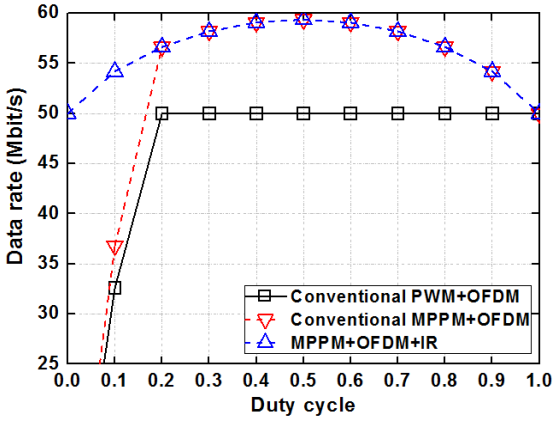

FIGURE 11. Comparison of the maximum achievable data rate with the total launching power limited to 10 W.

of κ. However, adopting larger κ will slightly degrade system performance when demodulating both MPPM and OFDM signals. This trade-off needs to be considered before system design. For the IR LED source, different values of κ almost have no influence on P_{tIR}. In order to further reduce P_{tIR}, the IR link with a larger modulation index can be used, as shown in Fig. 10. Since PDs designed for IR signals have been widely used, we can also adopt a PD with a larger responsivity in the IR waveband.

With the limited P_{tTotal} to be 10 W, Fig. 11 compares the maximum achievable data rate at different duty cycles. For all schemes and each dimming level in Fig. 11, 4-QAM is adopted and we assume m_{IR} to be 0.4. It can be observed that for all schemes, data rates larger than 50 Mbps can be always achieved for $0.3 \leq D \leq 1$. Conventional schemes with MPPM can offer higher capacity than PWM, reaching the highest data rate of ~60 Mbps with D to be 0.5. However, for $0 \leq D \leq 0.2$, the maximum achievable data rates for conventional schemes must be reduced to maintain reliable communication quality. After adopting the proposed hybrid scheme, it will be feasible to achieve reliable transmission at

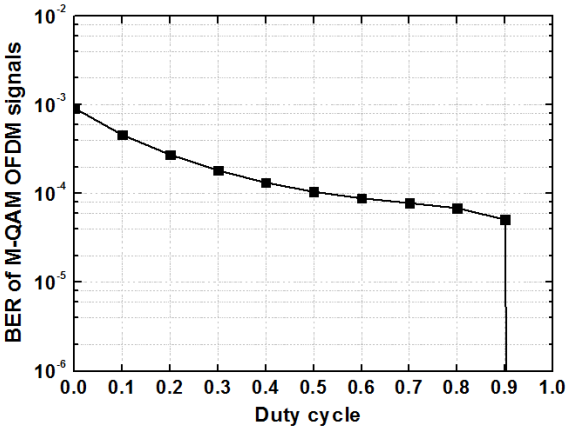

FIGURE 12. **BER performance of 4-QAM OFDM in the proposed hybrid scheme under different duty cycles.**

constant 50 Mbps within the full dimming levels from 1 to 0. Finally, Fig. 12 depicts the BER performance of the 4-QAM OFDM signal adopted in the hybrid system corresponding to Fig. 11. As can be observed, the optimum BER is achieved at D of 1 when there is only VL component. When conducting dimming control, with reduced dimming levels from 0.9 towards 0, the BER will slightly increase along with the growing proportion of addition IR transmission. However, reliable link quality can be eventually achieved within the full dimming control range, even at D of 0 when there is no VL signal transmission (i.e., the dark condition).

V. CONCLUSION

We propose a hybrid VL/IR transmission scheme for indoor VLC systems based on OFDM and MPPM dimming control. An additional low-power IR link is adopted to complement VL transmission. Compared with conventional schemes, our scheme is simple and power-efficient to satisfy the receiver sensitivity requirement, especially under low illumination levels. Simulation results reveal that when adopting the hybrid scheme, the required M-QAM level, required M-QAMsymbol rate, and total required LED launching power of VLC systems can be effectively reduced at a constant transmission rate with BER $<10^{-3}$. Even with limited LED transmit power, reliable communication at a constant data rate can still be guaranteed under all dimming levels between 1 and 0. In our future work, we will verify the performance of the proposed hybrid transmission scheme by experiments and investigate on the potential integration with IR uplink solutions.

REFERENCES

[1] E. F. Schubert and J. K. Kim, "Solid-state light sources getting smart," *Science*, vol. 308, no. 5726, pp. 1274–1278, May 2005.

[2] M. H. Crawford, "LEDs for solid-state lighting: Performance challenges and recent advances," *IEEE J. Sel. Topics Quantum Electron.*, vol. 15, no. 4, pp. 1028–1040, Jul. 2009.

[3] A. Sevincer, A. Bhattarai, M. Bilgi, M. Yuksel, and N. Pala, "LIGHTNETs: Smart lighting and mobile optical wireless networks—A survey," *IEEE Commun. Surveys Tuts.*, vol. 15, no. 4, pp. 1620–1641, 4th Quart., 2013.

[4] J. Grubor, S. Randel, K.-D. Langer, and J. Walewski, "Broadband information broadcasting using LED-based interior lighting," *J. Lightw. Technol.*, vol. 26, no. 24, pp. 3883–3892, Dec. 15, 2008.

[5] T. Komine and M. Nakagawa, "Fundamental analysis for visible-light communication system using LED lights," *IEEE Trans. Consum. Electron.*, vol. 50, no. 1, pp. 100–107, Feb. 2004.

[6] I. Din and H. Kim, "Energy-efficient brightness control and data transmission for visible light communication," *IEEE Photon. Technol. Lett.*, vol. 26, no. 8, pp. 781–784, Apr. 15, 2014.

[7] F. Zafar, D. Karunatilake, and R. Parthiban, "Dimming schemes for visible light communication: The state of research," *IEEE Wireless Commun.*, vol. 22, no. 2, pp. 29–35, Apr. 2015.

[8] K. Lee and H. Park, "Modulations for visible light communications with dimming control," *IEEE Photon. Technol. Lett.*, vol. 23, no. 16, pp. 1136–1138, Aug. 15, 2011.

[9] Y. Gu, N. Narendran, T. Dong, and H. Wu, "Spectral and luminous efficacy change of high-power LEDs under different dimming methods," *Proc. SPIE*, vol. 6337, pp. 63370J-1–63370J-7, Sep. 2006.

[10] J.-H. Choi, E.-B. Cho, T.-G. Kang, and C. G. Lee, "Pulse width modulation based signal format for visible light communications," in *OECC Tech. Dig.*, Jul. 2010, pp. 276–277.

[11] S. Rajagopal, R. D. Roberts, and S.-K. Lim, "IEEE 802.15.7 visible light communication: Modulation schemes and dimming support," *IEEE Commun. Mag.*, vol. 50, no. 3, pp. 72–82, Mar. 2011.

[12] J.-H. Choi, E.-B. Cho, Z. Ghassemlooy, S. Kim, and C. G. Lee, "Visible light communications employing PPM and PWM formats for simultaneous data transmission and dimming," *Opt. Quantum Electron.*, vol. 47, no. 3, pp. 561–574, May 2014.

[13] G. Ntogari, T. Kamalakis, J. Walewski, and T. Sphicopoulos, "Combining illumination dimming based on pulse-width modulation with visible-light communications based on discrete multitone," *IEEE J. Opt. Commun. Netw.*, vol. 3, no. 1, pp. 56–65, Jan. 2011.

[14] Z. Wang, W.-D. Zhong, C. Yu, J. Chen, C. P. S. Francois, and W. Chen, "Performance of dimming control scheme in visible light communication system," *Opt. Express*, vol. 20, no. 7, pp. 18861–18868, Aug. 2012.

[15] H. Elgala and T. D. Little, "Reverse polarity optical-OFDM (RPO-OFDM): Dimming compatible OFDM for gigabit VLC links," *Opt. Express*, vol. 21, no. 20, pp. 24288–24299, 2013.

[16] A. B. Siddique and M. Tahir, "Joint rate-brightness control using variable rate MPPM for LED based visible light communication systems," *IEEE Trans. Wireless Commun.*, vol. 12, no. 9, pp. 4604–4611, Sep. 2013.

[17] Y. Zeng, R. Green, and M. Leeson, "Multiple pulse amplitude and position modulation for the optical wireless channel," in *Proc. IEEE ICTON*, Jun. 2008, pp. 193–196.

[18] A. B. Siddique and M. Tahir, "Bandwidth efficient multi-level MPPM encoding decoding algorithms for joint brightness-rate control in VLC systems," in *Proc. IEEE GLOBECOM*, Dec. 2014, pp. 2143–2147.

[19] X. You, J. Chen, H. Zheng, and C. Yu, "Efficient data transmission using MPPM dimming control in indoor visible light communication," *IEEE Photon. J.*, vol. 7, no. 4, Aug. 2015, Art. no. 7902512.

[20] H. Le Minh *et al.*, "100-Mb/s NRZ visible light communications using a postequalized white LED," *IEEE Photon. Technol. Lett.*, vol. 21, no. 15, pp. 1063–1065, Aug. 1, 2009.

[21] H. Li, X. Chen, B. Huang, D. Tang, and H. Chen, "High bandwidth visible light communications based on a post-equalization circuit," *IEEE Photon. Technol. Lett.*, vol. 26, no. 2, pp. 119–122, Jan. 15, 2014.

[22] J. Armstrong, "OFDM for optical communications," *J. Lightw. Technol.*, vol. 27, no. 3, pp. 189–204, Feb. 1, 2009.

[23] J. Armstrong and B. Schmidt, "Comparison of asymmetrically clipped optical OFDM and DC-biased optical OFDM in AWGN," *IEEE Commun. Lett.*, vol. 12, no. 5, pp. 343–345, May 2008.

[24] H. Elgala, R. Mesleh, and H. Haas, "Indoor broadcasting via white LEDs and OFDM," *IEEE Trans. Consum. Electron.*, vol. 55, no. 3, pp. 1127–1134, Aug. 2009.

[25] H. Sugiyama and K. Nosu, "MPPM: A method for improving the band-utilization efficiency in optical PPM," *J. Lightw. Technol.*, vol. 7, no. 3, pp. 465–472, Mar. 1989.

[26] *Safety of Laser Products—Part 1: Equipment Classification and Requirements*, International Standard IEC 60825-1, 2014.

[27] *Photobiological Safety of Lamps and Lamp Systems*, International Standard IEC 62471, 2006.

[28] C. W. Oh, Z. Cao, E. Tangdiongga, and T. Koonen, "Free-space transmission with passive 2D beam steering for multi-gigabit-per-second per-beam indoor optical wireless networks," *Opt. Express*, vol. 24, no. 17, pp. 19211–19227, Aug. 2016.
[29] T. Koonen, J. Oh, K. Mekonnen, Z. Cao, and E. Tangdiongga, "Ultra-high capacity indoor optical wireless communication using 2D-steered pencil beams," *J. Lightw. Technol.*, vol. 34, no. 20, pp. 4802–4809, Oct. 15, 2016.
[30] J. M. Kahn and J. R. Barry, "Wireless infrared communications," *Proc. IEEE*, vol. 85, no. 2, pp. 265–298, Feb. 1997.
[31] F. E. Alsaadi, M. A. Alhartomi, and J. M. H. Elmirghani, "Fast and efficient adaptation algorithms for multi-gigabit wireless infrared systems," *J. Lightw. Technol.*, vol. 31, no. 23, pp. 3735–3751, Dec. 1, 2013.
[32] Z. Ghassemlooy, W. Popoola, and S. Rajbhandari, *Optical Wireless Communications: System and Channel Modelling With MATLAB*. Boca Raton, FL, USA: CRC Press, 2012, pp. 21–25.
[33] P. D. Diamantoulakis and G. K. Karagiannidis, "Simultaneous lightwave information and power transfer (SLIPT) for indoor IoT applications," in *Proc. IEEE GLOBECOM*, Dec. 2017, pp. 1–6.
[34] D. Karunatilaka, F. Zafar, V. Kalavally, and R. Parthiban, "LED based indoor visible light communications: State of the art," *IEEE Commun. Surveys Tuts.*, vol. 17, no. 3, pp. 1649–1678, 3rd Quart., 2015.
[35] A. Burton, E. Bentley, H. Le Minh, Z. Ghassemlooy, N. Aslam, and S.-K. Liaw, "Experimental demonstration of a 10Base-T Ethernet visible light communications system using white phosphor light-emitting diodes," *IET Circuits, Devices Syst.*, vol. 8, no. 4, pp. 322–330, Jul. 2014.
[36] X. You, J. Chen, C. Yu, and Z. Ghassemlooy, "Efficient transmission under low dimming control levels in indoor visible light communications," in *Proc. IEEE CSNDSP*, Jul. 2016, pp. 1–5.
[37] L. Zeng *et al.*, "High data rate multiple input multiple output (MIMO) optical wireless communications using white LED lighting," *IEEE J. Sel. Areas Commun.*, vol. 27, no. 9, pp. 1654–1662, Dec. 2009.
[38] Z. Wang, C. Yu, W.-D. Zhong, J. Chen, and W. Chen, "Performance of a novel LED lamp arrangement to reduce SNR fluctuation for multi-user visible light communication systems," *Opt. Express*, vol. 20, no. 4, pp. 4564–4573, Jun. 2012.
[39] A. J. Goldsmith and S.-G. Chua, "Variable-rate variable-power MQAM for fading channels," *IEEE Trans. Commun.*, vol. 45, no. 10, pp. 1218–1230, Oct. 1997.
[40] R. Essiambre, G. Kramer, P. J. Winzer, G. J. Foschini, and B. Goebel, "Capacity limits of optical fiber networks," *J. Lightw. Technol.*, vol. 28, no. 4, pp. 662–701, Feb. 15, 2010.
[41] D. Tsonev and H. Haas, "Avoiding spectral efficiency loss in unipolar OFDM for optical wireless communication," in *Proc. IEEE ICC*, Jun. 2014, pp. 3336–3341.
[42] S. D. Dissanayake, K. Panta, and J. Armstrong, "A novel technique to simultaneously transmit ACO-OFDM and DCO-OFDM in IM/DD systems," in *Proc. GLOBECOM Workshops*, Dec. 2012, pp. 782–786.
[43] R. C. Kizilirmak and Y. H. Kho, "Mitigation of illumination interference caused by PWM dimming in OFDM based visible light communication systems," in *Proc. IEEE I4CT*, Apr. 2015, pp. 489–492.
[44] J. Canny, "A computational approach to edge detection," *IEEE Trans. Pattern Anal. Mach. Intell.*, vol. PAMI-8, no. 6, pp. 679–698, Nov. 1986.
[45] K. Lee, H. Park, and J. R. Barry, "Indoor channel characteristics for visible light communications," *IEEE Commun. Lett.*, vol. 15, no. 2, pp. 217–219, Feb. 2011.
[46] E. Sarbazi, M. Uysal, M. Abdallah, and K. Qaraqe, "Indoor channel modelling and characterization for visible light communications," in *Proc. IEEE ICTON*, Jul. 2014, pp. 1–4.

XIAODI YOU received the B.S. and Ph.D. degrees in information and communication engineering from the Nanjing University of Posts and Telecommunications (NJUPT), Nanjing, China, in 2013 and 2018, respectively. He was with the School of Telecommunications and Information Engineering, NJUPT. He has been with the Department of Electronic and Information Engineering, The Hong Kong Polytechnic University, as a Post-Doctoral Research Associate since 2018. His research interests include visible light communication and coherent optical communication.

JIAN CHEN received the B.S., M.S., and Ph.D. degrees in electronic engineering from Southeast University, Nanjing, China, in 1988, 1990, and 1994, respectively. From 1994 to 1999, he was an Associate Professor with the Department of Communications, Nanjing University of Posts and Telecommunications (NJUPT). From 1999 to 2001, he was with the Department of Electrical Engineering, Korea Advanced Institute of Science and Technology, Daejeon, South Korea. In 2002, he was a member of the Technical Staff with the Institute for Communication Research, National University of Singapore. Since 2003, he has been a Research Scientist with the RF and Optical Department, Institute of Infocomm Research, Agency for Science, Technology and Research, Singapore. Since 2010, he has been a Full Professor with NJUPT. His research interests include coherent optical communication, visible light communication, and optical access networks.

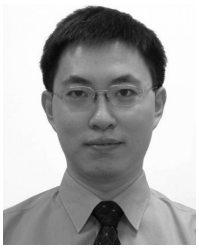

CHANGYUAN YU received the B.S. degree in applied physics and the B.Ec. degree in management from Tsinghua University, Beijing, China, both in 1997, the M.S. degree in electrical and computer engineering from the University of Miami, Coral Gables, FL, USA, in 1999, and the Ph.D. degree in electrical engineering from the University of Southern California, Los Angeles, CA, USA, in 2005. In 2005, he was a Visiting Researcher with NEC Labs America, Princeton, NJ, USA. He then joined the Faculty of the National University of Singapore in 2005 and served as the Founding Leader for the Photonic System Research Group, Department of Electrical and Computer Engineering. He was also a Joint Senior Scientist with the A*STAR Institute for Infocomm Research in 2005. In 2015, he joined the Department of Electronic and Information Engineering, The Hong Kong Polytechnic University, as an Associate Professor. His research interests include photonic devices, subsystems, optical fiber communication, sensor systems, and biomedical instruments. He has authored or co-authored one U.S. patent, six book chapters, and over 388 journal and conference papers (75 invited, including OFC2012 in USA). He has served as Technical Program Committee (TPC) or organizing committee for 80+international conferences (including a TPC member of OFC2014-2016, the General Chair of SPPCom2015, and the TPC Chair of SPPCom2014 in USA).